

A Kruskal-like Model with Finite Density¹

Charles Hellaby

Department of Applied Mathematics, University of Cape Town, Rondebosch 7700, South Africa

Classical and Quantum Gravity **4**, 635-50 (1987)

(Received 28 May 1986, in final form 7 October 1986)

Abstract

The Novikov coordinates for the Kruskal-Schwarzschild spacetime are derived from the Tolman model and generalised. It is then shown that models with identical two-sheets-and-a-neck topologies can have a non-zero density and that other unusual topologies are possible for Tolman models. The introduction of matter into such a model is found to split the horizons in the two sheets, and to reduce communication between them. The topology of the neck always requires paired white and black holes, which in these models are the big bang and big crunch singularities. It is concluded that worm holes between universes can exist in cosmological (i.e. dynamic, non-vacuum) models also.

1. Introduction

Although the Tolman² model has been known for more than 50 years, it has mostly been used to describe inhomogeneities in asymptotically homogeneous or empty spacetimes. In fact, even the description of a simple closed model, analogous to the closed Robertson-Walker models, was not really attempted before Zel'dovich and Grishchuk (1984) pointed out that a maximum in the areal radius, R , must be present in any spacelike section. Certainly, the full range of topological possibilities in Tolman models has not been explored.

The models to be considered are all Tolman models and it is assumed that they must have neither shell crossings nor surface layers, since these are not present in the Schwarzschild-Kruskal model.

2. The Tolman Model

The Tolman model (Lemaître 1933, Tolman 1934, Datt 1938, Bondi 1947) represents a distribution of pressure-free matter (i.e. dust) that is spherically symmetric, but inhomogeneous in the radial direction, and it is written in synchronous comoving coordinates. The cosmological constant, Λ , is set to zero and geometric units are used. The metric is

$$ds^2 = -dt^2 + \frac{R'^2}{1+f} dr^2 + R^2 d\Omega^2, \quad (2.1)$$

where $d\Omega^2 = d\theta^2 + \sin^2\theta d\phi^2$, $' \equiv \partial/\partial r$ and $\dot{} \equiv \partial/\partial t$ will be used below. The evolution of the areal radius, $R(r, t)$, is, from Einstein's equations,

$$\dot{R}^2 = \frac{F}{R} + f, \quad (2.2)$$

¹Post-publication: A few sentences have been edited for clarity. Actual errors are noted separately.

²Post-publication: These days I would call it the "Lemaître-Tolman" model. Many prefer "Lemaître-Tolman-Bondi".

while the density is³

$$8\pi\rho = \frac{F'}{R^2 R'} . \quad (2.3)$$

Eq (2.2) has the three solutions:

hyperbolic, $f > 0$,

$$R = \frac{F}{2f}(\cosh \eta - 1) , \quad (\sinh \eta - \eta) = \frac{2f^{3/2}(t - a)}{F} ; \quad (2.4)$$

parabolic, $f = 0$,

$$R = \left(\frac{9F(t - a)^2}{4} \right)^{1/3} ; \quad (2.5)$$

and elliptic, $f < 0$,

$$R = \frac{F}{2(-f)}(1 - \cos \eta) , \quad (\eta - \sin \eta) = \frac{2(-f)^{3/2}(t - a)}{F} . \quad (2.6)$$

These three types of time evolution correspond to the three types in Robertson-Walker models. The Tolman models contain three arbitrary functions of coordinate radius, r . The effective gravitational mass within radius r is $F(r)/2$, while $a(r)$ is the big bang time — the time at which $R = 0$ locally. (This assumes we take $t > a$ above.) The function $f(r)$ is a kind of local energy constant which determines the type of time evolution, but its geometrical role is discussed below. The time reverse of the above equations are also possible solutions, in which case $a(r)$ is the time of the big crunch, and the hyperbolic and parabolic cases are collapsing models.

In a closed model there must be two origins, i.e. two values of r where $R(r = \text{constant}, t) = 0$ for all t , and in between there must be a maximum where $R'(r = \text{constant}, t) = 0$ for all t . Such a maximum must be comoving, and must occur where $f = -1$, if there are to be no surface layers (see Zel'dovich and Grishchuk 1984, Hellaby and Lake 1985). This is also true for a minimum in R . Any other surface on which $R' = 0$ is a shell crossing (or possibly the big bang if $a' = 0$). Shell crossings are an undesirable feature of any realistic model and the conditions for avoiding them were derived previously (Hellaby and Lake 1985, but note that the symbols R and r are swapped in that paper). For convenience, the conditions for no shell crossings or surface layers have been summarised in the appendix, using the current notation.

3. The Geometrical Significance of $f(r)$

Robertson-Walker (RW) models with a dust equation of state, are easily derived from (2.1)-(2.6), by setting $a(r) = 0$, and $f(r) \sim F(r)^{2/3}$. Figure 1 shows the embedding of a 2D section, $t = \text{constant}$, $\theta = \pi/2$, of a closed RW model. If ψ is defined by

$$f(r) = -\cos^2 \psi , \quad (3.1)$$

then it gives the angle of the tangent cone at $r = \cos \psi$.

In the more general case of the Tolman model (TM), where the curvature is not uniform, the interpretation (3.1) may still be used⁴, see figure 2. If the value of f were held constant, the resulting 2D spatial sections would be cones of angle ψ . The above two examples both have negative values of f , but positive values may be interpreted in terms of hypercones such that the 'angle' is given by

$$f(r) = \cosh^2 \psi . \quad (3.2)$$

³Post-publication: These days I would use $2M(r)$ rather than $F(r)$.

⁴Post-publication: However we no longer have $r = \cos \psi$.

It is apparent then, that once the conditions for no shell crossings have been satisfied, the geometry of the spatial sections is determined solely by $f(r)$. This same function also determines the type of time evolution at each point. Later on we take advantage of the role of $f(r)$ to construct a variety of topologies.

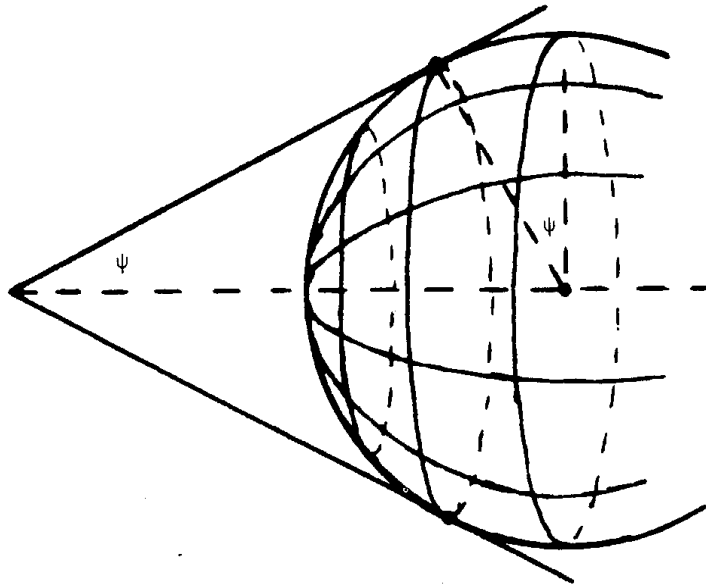


Figure 1. Embedding of a two-dimensional spatial section of the Robertson-Walker model ($t = \text{constant}$, $\theta = \pi/2$), showing the tangent cone at $r = \cos \psi$.

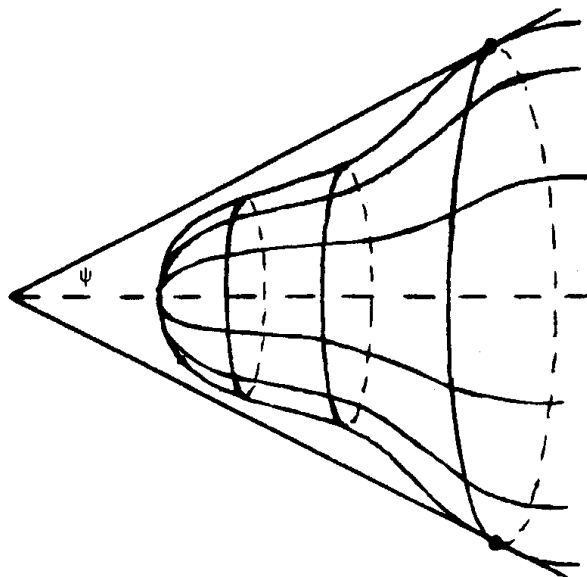


Figure 2. Embedding of a corresponding section of an elliptic Tolman model, showing a tangent cone.

4. Novikov Coordinates

Novikov coordinates (Novikov 1963, but see Landau and Lifshitz 1975, Misner et al 1973) are a much neglected representation of the Schwarzschild model, using Tolman (T)-like coordinates. They represent the spacetime as dynamic, using evolution functions that are familiar from the RW and T models. They have several advantages; they clearly show the past and future singularities, the

r and t coordinates are spacelike and timelike everywhere, and they make the topological structure quite obvious. Also the horizons are not at all singular in these coordinates. In fact the difficulty of deriving their loci explicitly rather than implicitly is the only disadvantage.

Any TM with⁵ $F' = 0$ is a vacuum model, by (2.3), and so must be at least a part of the Kruskal⁶ spacetime, but the full Kruskal manifold (KM) (see Misner et al 1973, pp 835-9) is not always obtained by a given choice of arbitrary functions. In order to obtain the Novikov coordinates (or similar ones), which cover the full manifold, the following choices are made for the three arbitrary functions.

(i) Set $F(r) = \text{constant}$, so that the density is zero.

(ii) The symmetry between the past and future singularities of the KM suggests choosing the bang and crunch singularities to be reflections of each other about the axis $t = 0$, as follows:

$$a = \frac{-\pi F}{2(-f)^{3/2}} \quad . \quad (4.1)$$

This means $t = 0$ is a simultaneous time of maximum expansion.

(iii) The Kruskal (K) topology — of two asymptotically flat sheets joined by a neck — requires that, on any spacelike surface (that does not intersect the bang or crunch), the areal radius R should decrease from infinity at $r = -\infty$, to a minimum value at $r = 0$, say, and increase again to infinity as $r \rightarrow \infty$. This is achieved by choosing $f(r) = -1$ at the minimum (where $R' = 0$) to avoid a surface layer and letting it rise asymptotically to zero in either direction. The asymptotic value of zero is suggested by the requirement for asymptotic flatness at spatial infinity.

These choices are sketched in figure 3. They ensure there are no shell crossings even though the exact form of $f(r)$ has not yet been specified. The particular choice of $f(r)$ is unimportant, as long as it monotonically increases from -1 to 0 in either direction from $r = 0$. The r, t diagram for Novikov coordinates (Landau and Lifshitz 1975) is similar to the Kruskal diagram. The vertical lines ($r = \text{constant}$) are obviously geodesics of the spacetime and in the Penrose diagram they would appear as in figure 4.

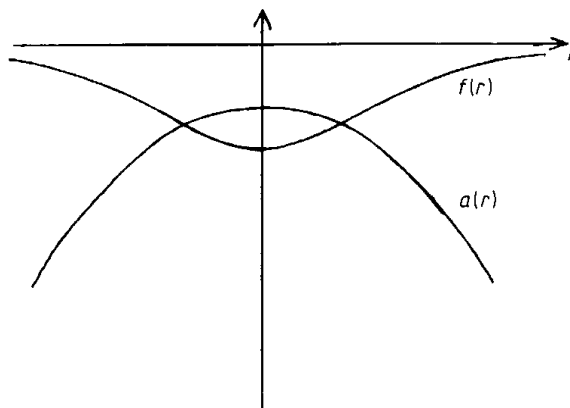


Figure 3. Sketch of $f(r)$ and $a(r)$ for Novikov-like coordinates. The vertical scale is not necessarily the same for both curves.

⁵Post publication: i.e. $F = \text{constant}$. The published version mistakenly had $F' = \text{constant}$ here.

⁶Post-publication: i.e. Kruskal-Szekeres.

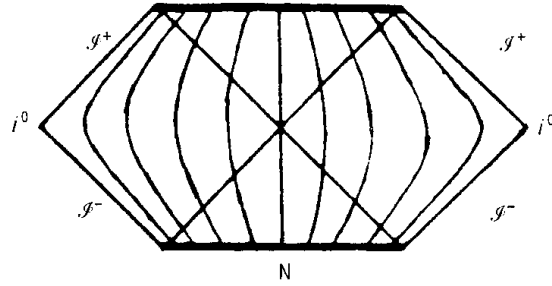


Figure 4. Sketch of the Penrose diagram for Kruskal space showing the lines of constant r of Novikov coordinates.

5. Other Coordinate Systems

The above requirements are, in fact, stronger than is necessary for a full manifold with $F' = \text{constant}$. One feature which is essential, though, is the minimum value of $f = -1$ at the neck. Since both F' and f' are zero here, $a' = 0$ is forced in order to avoid shell crossings, as well as by the requirements for no surface layers. The same conditions also show that $f' \geq 0$ is necessary wherever $R' > 0$ and vice versa. (This means that, in vacuum, there cannot be another minimum or maximum in $R(r, t = \text{constant})$ without creating a surface layer, since f cannot reach -1 again.) An inflection point in f , and therefore in a and in R , may also be excluded as merely causing degenerate coordinates. Therefore $f' = 0$ is not allowed away from $r = 0$.

Though f must be monotonically increasing, its asymptotic value does not have to be 0, though a negative value is not possible. In the latter case it is obvious from (2.6) that R would approach a maximum value in the radial direction, so the manifold would be incomplete and r would become degenerate. The case of a positive asymptotic value of f , the particular spatial sections, $t = \text{constant}$, would have negative curvature. But none of the conditions prevent this choice, and since $F' = 0$, it must represent the KM. This can be understood by noting that the $r = \text{constant}$ lines are again geodesics of the spacetime, but in this case some of the geodesics chosen are those with sufficient energy to escape to infinity.

The various possibilities for coordinate coverage of the Penrose diagram are shown in the sketches in figure 5. In these diagrams only one of the sheets of the spacetime is shown and N represents the location of the neck. This is done because there is no reason why the coordinate coverage of the two sheets should be mirror symmetric about $r = 0$. We could join one of the diagrams below to the reflection of any of the three.

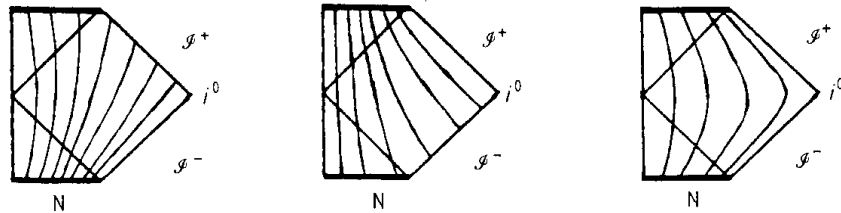


Figure 5. Some possibilities for coordinate coverage of the Kruskal manifold using different Tolman models. N is the location of the neck.

Since both past and future singularities in the KM are entirely spacelike, a valid coordinate system could represent either of them as simultaneous. The bang and crunch surfaces in TMs are likewise always spacelike, so this puts no restriction on the choice of $a(r)$. However, because $f(r)$ approaches a zero or positive value at finite or large r , at least one of the surfaces must go to infinity,

or minus infinity, because the time from bang to crunch diverges as a negative f approaches zero. But the conditions for no shell crossings do require the bang surface to obey $a' \leq 0$ for $R' > 0$ and vice versa. (If $t = a$ is chosen to be the crunch surface, then the converse must hold.) This is the only restriction on $a(r)$. Note, however, that condition (4.1) is not essential, and indeed it cannot be maintained in a model where f becomes ≥ 0 at finite r . Nevertheless, the lack of time symmetry in the coordinates does not mean the spacetime has lost its symmetry. Again, variations in the choice of $a(r)$ merely represent variations in the particular geodesics chosen to cover the spacetime.

The purpose of all of the above is to help ascertain what is and is not different in the models below.

6. A Dense Model

It is clear from the above discussion that what gives the two-sheet topology is the choice of the function $f(r)$, while the choice $F' = 0$, gives vacuum. In fact, if we ask a different question, what kind of spacetime can we get if we consider a TM with $F = \text{constant}$, then it is found from (2.4)-(2.6) that no origin (as defined in §2) is possible, and so the only way to get a complete manifold is to go through a neck and out into another sheet. Thus the choice of constant F forces the K topology, but the reverse is not true. We may choose $f(r)$ to be as above, and still keep F' non-zero, so that there is finite density throughout the spacetime. Such a model is given by the following arbitrary functions:

$$F = F_0 \alpha^n, \quad F_0, n \geq 0, \quad (6.1a)$$

$$f = \frac{-1}{\alpha}, \quad (6.1b)$$

$$a = \frac{-\pi F}{2(-f)^{3/2}} = \frac{-\pi F_0 \alpha^{(n+3/2)}}{2}, \quad (6.1c)$$

where the function $\alpha(r)$ is even about $r = 0$, has a minimum of $+1$ at $r = 0$, and rises monotonically to infinity in either direction. It can easily be checked that there are no shell crossings or surface layers. Consequently, the density is non-zero everywhere, including at the neck, but dies away towards spatial infinity on both sheets. In this model, unlike the case of vacuum, the spacetime is everywhere dynamic. The matter is thrown out of the white hole initially, but none of it has enough energy to escape, so it all eventually collapses into the black hole. The model is meant to be as similar to the K spacetime as possible, except for having finite density, and its r, t diagram is very much like the Kruskal diagram. It is apparent from the form of $f(r)$ that it has the neck-and-two-sheets topology and it also has the same time symmetry, as well as being asymptotically flat. On the spatial sections, the mass function, F , decreases to a minimum value at the neck, and then increases outwards in the second sheet. The presence of matter obviously affects the detailed geometry, but it does not affect the topological structure. The KM is a special case of this set of models, having $n = 0$.

7. The Range of Possibilities

There are many other possible topologies for TMs. Firstly, we could take all of the types of coordinate coverage given above in figure 5 and add in a non-zero density. Now the coordinate lines become particle paths, and in general the time symmetry is lost. Thus we could have a model in which some of the matter thrown out of the white hole escapes to infinity, or one in which some of the matter falling into the black hole is accreted from infinity. And it is perfectly possible to have different behaviours for the matter in each sheet — for example, expulsion of matter in one sheet and accretion in the other (see the explicit example below).

All of these models must have zero density at infinity. If the density remains finite out to

infinity, then the conformal structure of infinity cannot be as shown in those diagrams. Instead, it could be like the structure of a RW model. Note that, since F' may now be non-zero, negative asymptotic values of f at large r become possible. Thus, other possibilities for the Penrose diagram are as shown below in figure 6.

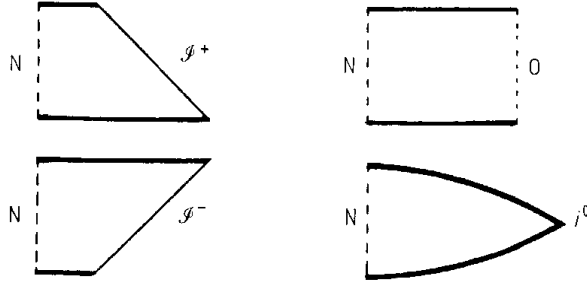


Figure 6. Some possible Penrose diagrams for Tolman models having a neck in the spatial sections at N . O is the location of an origin.

The two on the left could represent asymptotically parabolic or hyperbolic sheets. Once matter is present, the latter can no longer be asymptotically flat. The top right one represents a completely elliptic sheet that is spatially semi-closed and the bottom right one shows a completely elliptic model that is open. It has spatial infinity, but no null infinity. In the semi-closed case, the areal radius R on the spatial sections increases away from the neck, until it reaches a maximum, and then decreases to zero, thus closing off the space with an origin, marked by O . Obviously, in this example, $f = -1$ is required at the maximum, and beyond it $R' < 0$, $F' < 0$, $a' > 0$, and $f' > 0$ must obtain. (If both sheets are semi-closed, then the model is truly closed.)

In what follows, it will be seen that the topological constructions of Sussman (1985) can be realised in a more natural way, using single non-empty Tolman models.

8. The String of Beads Model

The previous example illustrates another possibility in finite density models that was not possible with vacuum. Since F' is different from zero, the conditions for no shell crossings no longer imply $f' \geq 0$ where $R' > 0$. In order to go from the neck to the maximum in R in that example, it is necessary for $f(r)$ to rise from -1 , and then decrease to it again. Now if both sheets were elliptic, it would then be possible to go from a maximum in R , to a minimum at the neck, and out to a maximum again. Evidently it is possible to extend this sequence indefinitely, so creating an infinite series of necks and bellies in the spatial sections. An example of such a model is given by the following functions:

$$F = F_0 + F_1 \cos r \quad , \quad F_0 > F_1 > 0 \quad , \quad (8.1a)$$

$$f = -(1 - f_1 \sin^2 r) \quad , \quad 1 > f_1 > 0 \quad , \quad (8.1b)$$

$$a = \frac{-\pi F}{2(-f)^{3/2}} = \frac{-\pi(F_0 + F_1 \cos r)}{(1 - f_1 \sin^2 r)^{3/2}} \quad . \quad (8.1c)$$

For f_1 small enough there are neither surface layers nor shell crossings and the density is non-zero everywhere. Consider the embedding of the usual 2D spatial slices. This spacetime starts off as an infinite row of unconnected bubbles with white holes at either side, which grow till they join. The necks expand for a while, then shrink and pinch off, leaving a row of contracting bubbles having two black holes each. The meaning of the limit on f , is that the necks may not be too narrow compared with the bellies. The model has the following r, t diagram, and Penrose diagram.

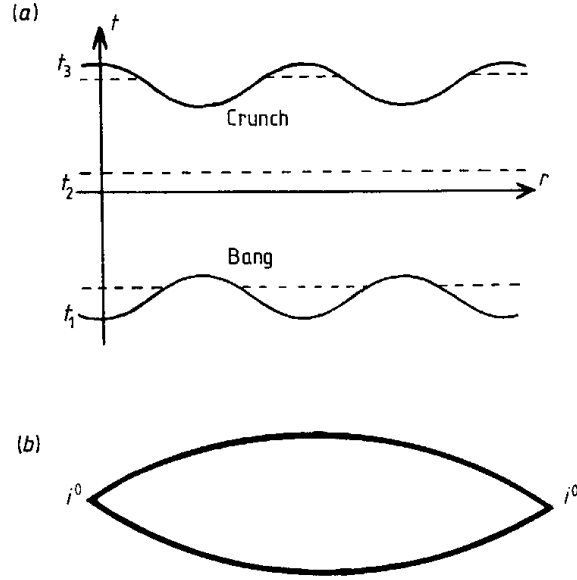


Figure 7. (a) The r, t diagram for the above model. The matter flows along the vertical lines, $r = \text{constant}$. (Each point represents a two-dimensional surface, a spherical shell of matter.) At time t_1 there is an infinite string of expanding disconnected universes, at t_2 they are all linked by necks, and at t_3 they are split up again and are collapsing. (b) The Penrose diagram for the above model.

9. In One Ear and Out the Other

Consider the following model. In the range $r \geq 0$, take the region $t > a$ in (2.4)-(2.6) and the functions

$$F = F_0 + F_1 r^3, \quad F_0, F_1 > 0, \quad (9.1a)$$

$$f = -(1 - f_1 r^2), \quad f_1 > 0, \quad (9.1b)$$

$$a = -\frac{1}{2} F_0 \left(1 + \frac{3}{2} f_1 r^2\right), \quad (9.1c)$$

while in the range $r \leq 0$, take the region $t < a$, with the functions

$$F = F_0 - F_1 r^3, \quad (9.1d)$$

$$f = -(1 - f_1 r^2), \quad (9.1e)$$

$$a = \frac{1}{2} \pi F_0 \left(1 + \frac{3}{2} f_1 r^2\right). \quad (9.1f)$$

In (9.1c), $a(r)$ is the time of the bang, and the crunch happens at time $t = a + \pi F / (-f)^{3/2}$, while in (9.1f), $a(r)$ is the time of the crunch, and the bang happens at $t = a - \pi F / (-f)^{3/2}$. Thus the bang and crunch surfaces join smoothly at $r = 0$, as shown in figure 8. The join is C^1 , but could be made arbitrarily smooth by adding terms to (9.1c) and (9.1f). Again the density is finite everywhere, there are no shell crossings or surface layers and the model is asymptotically open and hyperbolic in both sheets.

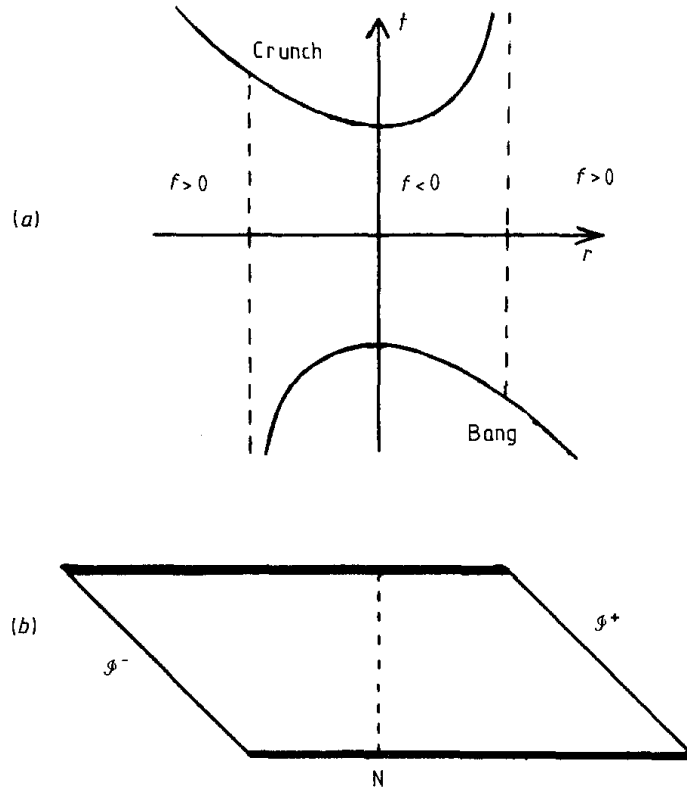


Figure 8. (a) The r, t diagram for the above model. The matter flows along the vertical lines, $r = \text{constant}$. The broken lines show where the time evolution is parabolic, $f = 0$. (b) The Penrose diagram for the above model.

In this model then, there is matter being thrown out of the white hole into an expanding hyperbolic spacetime in one sheet; there is an elliptic region near the neck, with matter flowing from past to future singularities, and in the second sheet matter is accreting onto the black hole from a collapsing hyperbolic spacetime.

10. The Essential Feature

The conditions for no shell crossings or surface layers are retained, so that the new models have the same continuity as the K space. The only remaining feature necessary to construct two sheet topologies with density is the condition for a neck, where $f = -1$, $F > 0$, F and f are at a minimum and a is at a maximum (or minimum if $t < a$).

There is one curious fact about this. Geodesics which pass through the minimum point in R certainly exist, but the material particles always have to be comoving with the minimum. Since there is no obvious physical process that would ensure this, it is possible that a more general model than the TM might allow particles to pass through the neck and flow from one sheet to the other.

11. Horizons

An obvious question is how the horizon structure is affected by the introduction of matter. In TMs the apparent horizon (AH) is the locus of points where the area of a wavefront of light is momentarily stationary and is given by

$$R = 2M = F \quad . \quad (11.1)$$

There is always one horizon for each singularity in the model, so the bang has a past AH (AH^-), where incoming rays are stationary, and the crunch has a future AH (AH^+). In the Kruskal case,

the event horizon is also an apparent horizon, while in the dense models, this is not in general true. Putting (11.1) in (2.4)-(2.6) gives the parametric solutions

$$f > 0 : \quad 2f = \cosh \eta - 1 ; \quad (11.2)$$

$$f = 0 : \quad 3(t - a) = 2F ; \quad (11.3)$$

$$f < 0 : \quad 2(-f) = 1 - \cos \eta ; \quad (11.4)$$

for the hyperbolic, parabolic and elliptic cases, respectively. In general there are two solutions to this equation along any given particle path (constant r) in an elliptic region, and one in a parabolic or hyperbolic region. But at the neck, the maximum value R reaches is F , so the two solutions must meet here. Since there is only one AH in hyperbolic regions, the second one in an elliptic region diverges towards infinite time as the parabolic point is approached, though it does not actually touch its singularity. In parabolic and hyperbolic regions, the AH becomes further from the singularity as R increases. In elliptic regions, however, the AH may recede from, and reapproach the singularities, and in a semi-closed sheet they touch the singularities at the origin. In asymptotically flat models like the one in (6.1a)-(6.1c) and those of figure 5, the AHs have the same structure as the event horizons of the KM.

The future event horizon (EH^+) is the light ray that divides those observers who cannot escape the future singularity from those that can, and conversely for the past EH. To find their exact locations would require actual integrations in specific models. Models which are asymptotically flat and empty, as shown in figure 5, may have both past and future EHs, but it will be shown that the presence of matter in a model tends to hinder communication between the two sheets. This also means that the horizons (past and future) in sheet 1 are no longer coincident with the horizons in sheet 2 (see figure 9). In the more general models of figure 6, there can only be an EH for each point where the future singularity meets future null infinity, or vice versa. So there will be one in each asymptotically parabolic or hyperbolic sheet (with $F' \neq 0$), and none in each completely elliptic sheet.

The gradient of the AH is found by differentiation of (11.1):

$$\left. \frac{dt}{dr} \right|_{AH} = \frac{F' - R'}{\dot{R}} , \quad (11.5)$$

while the gradient of the radial null vectors is, from the metric (2.1),

$$\left. \frac{dt}{dr} \right|_n = \frac{\varepsilon R'}{(1+f)^{1/2}} , \quad \varepsilon = \pm 1 , \quad (11.6)$$

and the ray is outgoing if it is moving away from the neck (i.e. towards increasing $|r|$, assuming $r = 0$ at the neck). Along these rays it is found, using (2.2), that

$$\left. \frac{dR}{dt} \right|_n = \varepsilon \left(\frac{F}{R} + f \right)^{1/2} + \varepsilon (1+f)^{1/2} , \quad \varepsilon = \pm 1 , \quad (11.7)$$

where $\varepsilon = -1$ when $R < 0$, and

$$\left. \frac{dR}{dr} \right|_n = R' \left[1 + \varepsilon \varepsilon \left(\frac{F/R + f}{1+f} \right)^{1/2} \right] . \quad (11.8)$$

The orientation of the AH is found from the ratio of (11.5) and (11.6), using (11.1) and the equation of motion (2.2):

$$\frac{dt/dr|_{AH}}{dt/dr|_n} = \varepsilon \varepsilon \left(\frac{F'}{R'} - 1 \right) . \quad (11.9)$$

The past AH, where the incoming rays are stationary, becomes incoming null if

$$F' = 0 \quad , \quad (11.10)$$

and so the AH is only an EH in vacuum. If $F' > 0$, the past AH may be spacelike, outgoing null, or outgoing timelike, but never incoming timelike. (Here outgoing refers to motion with respect to the comoving fluid.) The converse holds for the future AH.

The derivatives in (11.7) and (11.8) show how the rays behave within the AH. Now \dot{R} and R' are finite everywhere except near $R = 0$, and since $-1 < f < \infty$, this means both derivatives are finite and greater than zero everywhere within $0 < R < F$. Thus their integrals are finite in that range. At $R = 0$,

$$\dot{R} = \left(\frac{F}{R} \right)^{1/2} \quad (11.11)$$

and

$$R' \approx -a' \left(\frac{F}{R} \right)^{1/2} \quad \text{if } a' \neq 0 \quad (11.12)$$

otherwise

$$R' \approx \frac{F'R}{3F} \quad . \quad (11.13)$$

Therefore the integrals of (11.7) and (11.8) can be evaluated to lowest order in R and they are finite even at small R . So it is evident that a light ray starting from the past singularity at $R = 0$ approaches arbitrarily close to $R = F$ in finite t and in finite r . Where $F' \neq 0$, it passes through the past AH in finite t and r . The same argument applies to the region between the future AH and the future singularity.

Consider the point, P , where the two AH meet, i.e. the moment of maximum expansion at the neck. There are three possibilities.

(a) If $F'/R' \neq 0$ here (i.e. $\rho \neq 0$), the two radial light rays that pass through this point enter the future AH as they leave the past AH. Thus they go from past to future singularities in finite time, as in figure 9(a). Clearly any event horizons that exist must end on one of the singularities.

(b) If $F'/R' = 0$ at P , then the rays through P remain on the locus $R = F$ until they reach a region where $F' \neq 0$. They then fall inside the respective AH and must reach the singularities in finite time. Again any EH that exists must end on a singularity. (See the example in figure 9(b). There one sheet is completely vacuum.)

(c) It is possible that although matter is present somewhere, one (but not both) of the light rays going along $R = F$ might not encounter any of it (see the example in figure 9(c)). In this case, the past AH in one sheet and the future AH in the other would become EHs along that single ray.

Thus it is demonstrated that if there is any matter at all in a dense Kruskal-like model, then communication between the two sheets cannot be better than the vacuum case. If there is matter in the elliptic region then no ray from \mathcal{J}^- in one sheet can reach \mathcal{J}^+ in the other sheet. The conformal diagrams for an asymptotically empty model, showing event horizons, are as in figures 9(d) (which corresponds to 9(a) and 9(b)) and 9(e) (corresponding to 9(c)).

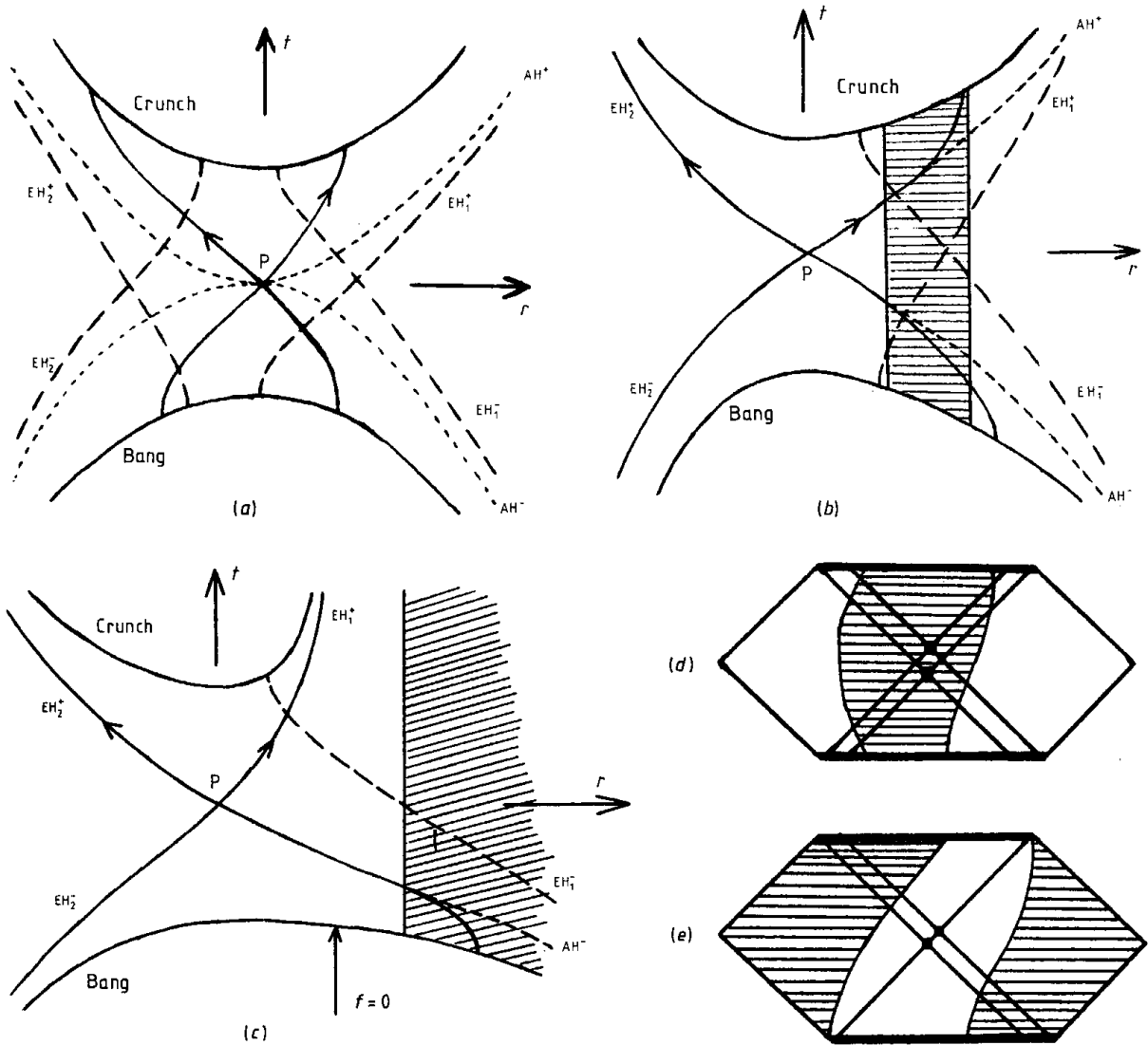


Figure 9. In (a), (b) and (c) the bold curves are the past and future singularities, the full curves are the light rays that pass through point P, the broken curves are event horizons and the dotted curves are apparent horizons. In (a) there must be matter at least around $r = 0$, but in (b) and (c) there is only vacuum outside the shaded areas. The two possible conformal diagrams for asymptotically empty models are shown in (d) and (e). There must be matter somewhere within the shaded part(s) of each diagram.

12. The Red-shift

Since the divergent blue-shift from white holes is a known instability of the Kruskal model, the red-shift behaviour of these modified models is of interest. The red-shift of geodesic emitters at the bang surface for non-empty Tolman models was worked out previously (Hellaby and Lake 1984) and the results hold for the general case here also. In brief, it was found that an infinite red-shift was the general result, while a divergent blue-shift occurred along radial rays from radial emitters only. There were also the 'forward rays' which show a finite frequency shift and which occur in the RW model as well. From the observer's point of view, they correspond to the emitter coming straight at him and are due to non-comoving emitters approaching light speed near the singularity. The emitter was approaching the velocity of the light ray which was just seen, so the effect does not depend on the observer's motion.

The general result for the red-shift of the past singularity in Schwarzschild models⁷ is a finite frequency shift. The well known divergent blue-shift is a forward ray effect and occurs along radial rays from radial emitters, as well as along forward rays in all other directions.

The introduction of matter seems to improve the red-shift behaviour of the model slightly, but it certainly makes it no worse.

13. Conclusions

Though the K topology is forced by the assumptions of spherical symmetry and vacuum, it is nevertheless not at all unique to vacuum, and the KM is only a special case of the more general two-sheet models.

As the parameter n in (6.1a)-(6.1c) is decreased to zero, the density at all events in that model smoothly approaches zero. This makes it clear that the KM has no material source for its curvature. There is no central particle that is responsible. Such a particle would have to follow a timelike world line, but it is evident that all observers see zero density, and there are no timelike singularities or discontinuities anywhere. The past and future singularities, being spacelike, do not represent the history of a particle and should be regarded as a bang and a crunch. Rather, the curvature is forced by the choice of topology and the gravitational field is due to the curvature. Thus it appears that a mass is close by. While Einstein's equations say that the presence of matter causes the curvature of the surrounding space, they do not guarantee the reverse. The curvature of space is not necessarily caused by the proximity of matter. This allows not only gravitational radiation, but also non-radiative models with unusual topologies.

Because all two-sheet Tolman models must be elliptic near the neck, none of them can have the two sheets connected for an infinite length of time. In other words, where there is a white hole, there must later be a black hole.

The term 'white hole' is often used to describe the gradual emergence of matter from the bang singularity in TMs with quite normal RW-like topologies. Aside from the topology, these are different from Schwarzschild white holes in that there is no associated event horizon. There is an apparent horizon, but its locus is quite different. However, in the models described here, which bridge the gap between the Schwarzschild model and the usual cosmological models, the distinction of having a Schwarzschild style event horizon is not possessed by all models with a neck.

The usual scenarios for collapse to a 'black hole' are also different. Since there is a central massive body at all times up to collapse, there is always a proper origin, and there is at no time a second sheet involved. The embedding diagram for such a model is shown in figure 10 for comparison with the Kruskal embedding. It is only when collapse has occurred that this 'black hole' is similar to one of the disconnected sheets of a Schwarzschild black hole. These other kinds of 'black holes' and 'white holes' do not have to come in pairs.

It is interesting to consider what an observer in the spacetime, who is watching the emergence of matter from the past singularity, would be able to deduce about the topology of his world. Until all the matter has emerged, it would not be obvious whether there was a neck and a second sheet to his world. In fact, since $f(r)$ is an arbitrary function, it would be utterly impossible to deduce it from any measurement. The usual argument for disallowing white holes (of all kinds) is that this unpredictability is not acceptable. It is worth pointing out that, whether the bang is simultaneous or not, an observer would always *see* a gradual emergence of matter from the bang, due to the longer light travel time from more distant parts of the singular surface. Viewed this way, the argument does not hold, since any infinite spacelike bang surface must continue to causally affect all observers

⁷i.e. vacuum TMs.

for ever.

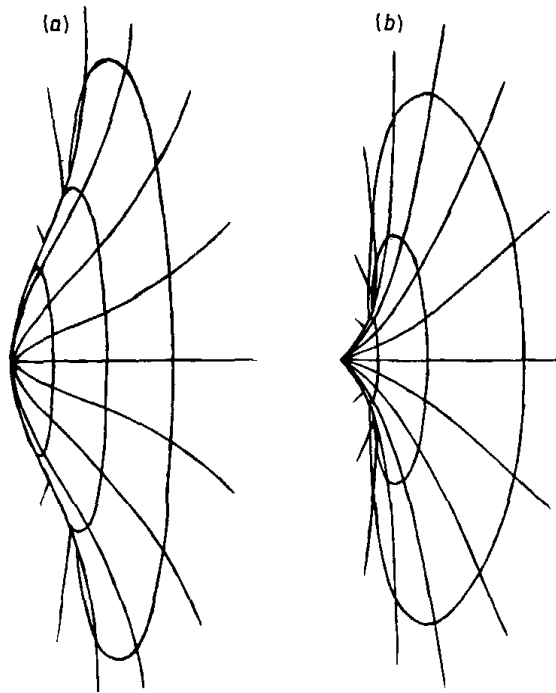


Figure 10. The embedding diagram for the usual collapse scenario, (a) before and (b) after collapse.

Since the dust RW model is obtained by a particular choice of the arbitrary functions, an inhomogeneous T region may be joined smoothly to a homogeneous RW region across any comoving spherical surface of constant r . If the T region is elliptic at the junction, then the RW region must have $k = +1$, and so on for the other cases. So two (or more) RW universes could be joined by one (or more) of these Tolman necks and the necks could be as narrow as desired. Similar sorts of constructions were described by Sussman (1985), but the above models have the advantage that the necks are not necessarily vacuum and they can be described by a single metric.

Acknowledgments

I would like to thank Bill Bonnor and George Ellis for helpful discussions.

Appendix

Some results from Hellaby and Lake (1985). The *conditions for no shell crossings* in Tolman models with $t > a$ are shown in the table below. If $t < a$, then a' should be replaced by $-a'$ throughout.

Table 1

	$F \geq 0$	$f < 0$
$R' > 0$	$a' \leq 0$ $f' \geq 0$ $F' \geq 0$ but no more than two equalities at once	$a' \leq 0$ $a' \geq \frac{-\pi F}{(-f)^{3/2}} \left(\frac{F'}{F} - \frac{3f'}{2f} \right)$ $F' \geq 0$ but not both $F' = 0$ and $f' = 0$ at once
$R' = 0$	$a' = 0$ $f' = 0$ $F' = 0$	$a' = 0$ $f' = 0$ $F' = 0$
$R' < 0$	$a' \geq 0$ $f' \leq 0$ $F' \leq 0$ but no more than two equalities at once	$a' \geq 0$ $a' \leq \frac{-\pi F}{(-f)^{3/2}} \left(\frac{F'}{F} - \frac{3f'}{2f} \right)$ $F' \leq 0$ but not both $F' = 0$ and $f' = 0$ at once

Assuming that the arbitrary functions are continuous, the *conditions for no surface layers* in Tolman models are that, where $R' = 0$, there are no shell crossings and $f(r) = -1$.

References

- Bondi H (1947) *Mon. Not. R. Astron. Soc.* **107** 410.
 Datt B (1938) *Z. Phys.* **108** 314.
 Hellaby C and Lake K (1984) *Astrophys. J.* **282** 1 (plus corrections in (1985) *Astrophys. J.* **294** 702).
 Hellaby C and Lake K (1985) *Astrophys. J.* **290** 381 (plus corrections in (1986) *Astrophys. J.* **300** 461).
 Landau L D and Lifshitz E M (1975) *The Classical Theory of Fields* (Oxford: Pergamon) pp 319-20.
 Lemaître G (1933) *Ann. Soc. Sci. Bruxelles* **A53** 51.
 Misner C W, Thorne K S and Wheeler J A (1973) *Gravitation* (San Francisco, CA: Freeman).
 Novikov I D (1963) *Doctoral Thesis* Shternberg State Astronomical Institute, Moscow.
 Sussman R A (1985) *Gen. Rel. Grav.* **17** 251.
 Tolman R C (1934) *Proc. Natl. Acad. Sci.* **20** 169.
 Zel'dovich Y B and Grishchuk L P (1984) *Mon. Not. R. Astron. Soc.* **207** 23 p.